

Investigation on synthesis and physical properties of metal doped picene solids

Takashi Kambe,^{1*} Xuexia He,² Yosuke Takahashi,¹ Yusuke Yamanari,¹ Kazuya Teranishi,² Hiroki Mitamura,², Seiji Shibasaki,¹ Keitaro Tomita,¹ Ritsuko Eguchi,² Hidenori Goto,^{2,6} Yasuhiro Takabayashi,² Takashi Kato,³ Akihiko Fujiwara,⁴ Toshikaze Kariyado,⁵ Hideo Aoki,⁵ and Yoshihiro Kubozono^{2,6*}

¹Department of Physics, Okayama University, Okayama 700-8530, Japan

²Research Laboratory for surface Science, Okayama University, Okayama 700-8530, Japan

³Institute for Innovative Science and Technology, Graduate School of Engineering, Nagasaki Institute of Applied Science, Nagasaki 851-0121, Japan

⁴Japan Synchrotron Radiation Research Institute, SPring-8, Hyogo 679-5198, Japan

⁵Department of Physics, The University of Tokyo, Hongo, Tokyo 113-0033, Japan

⁶Research Centre of New Functional Materials for Energy Production, Storage and Transport, Okayama University, Okayama 700-8530, Japan

PACS number; [74.70.Wz, 74.70.Kn, 74.62.Fj, 74.62.Bf]

(Received: 26 September 2012, Revised November 2012)

We report electronic structure and physical properties of metal-doped picene as well as selective synthesis of the phase that exhibits 18 K superconducting transition. First, Raman scattering is used to characterize the number of electrons

transferred from the dopants to picene molecules, where a softening of Raman scattering peaks enables us to determine the number of transferred electrons. From this we have identified that three electrons are transferred to each picene molecule in the superconducting doped picene solids. Second, we report pressure dependence of T_c in 7 K and 18 K phases of K_3 picene. The 7 K phase shows a negative pressure-dependence, while the 18 K phase exhibits a positive pressure-dependence which cannot be understood with a simple phonon mechanism of BCS superconductivity. Third, we report a new synthesis method for superconducting K_3 picene by a solution process with monomethylamine, CH_3NH_2 . This method enables us to prepare selectively the K_3 picene sample exhibiting 18 K superconducting transition. The method for preparing K_3 picene with $T_c = 18$ K found here may facilitate clarification of the mechanism of superconductivity.

Corresponding author: Takashi Kambe, kambe@cc.okayama-u.ac.jp & Yoshihiro Kubozono, kubozono@cc.okayama-u.ac.jp

I. Introduction

Recently a new class of organic superconductors has been discovered in aromatic systems. They are solids of hydrocarbons that include picene, coronene, phenanthrene and 1,2:8,9-dibenzopentacene,¹⁻⁶ doped with metal atoms. Namely, the superconductivity was first discovered in potassium-doped picene, K_3 picene, which showed two different superconducting transition temperatures, one with $T_c = 7$ K and the other as high as 18 K.¹ This has been followed by other studies, and the highest T_c among these hydrocarbon superconductors to date attains 33 K observed in $K_{3.45}$ dibenzopentacene,⁶ whose T_c is much higher than the highest T_c (14.2 K at 8.2 GPa⁷ in β - (BEDT-TTF)₂ICl₂) in charge-transfer organic superconductors. Thus the hydrocarbon superconductors are very attractive from viewpoints of development of new high- T_c superconductors as well as fundamental physics of superconductivity. Theoretical calculations for picene superconductors were also achieved, which suggests that the electron-phonon coupling is strong,^{8,9} the conduction band comprises four bands arising from two LUMO orbitals,¹⁰ and that strong hybridization between the dopants and molecules invalidates a rigid-band picture.¹⁰

The departure from the rigid-band picture was experimentally evidenced by photoemission spectroscopy.¹¹ This photoemission study clearly showed a metallic ground state for potassium-doped picene films. Our recent resistivity data also indicate a metallic behavior for the K_3 picene phase.¹² Further, a Pauli paramagnetic susceptibility was observed for a K_3 picene bulk sample.¹ These results support a metallic ground state for K_3 picene.

The T_c for the solid K_3 picene was found to be either 7 or 18 K,^{1,2} while the T_c of K_3 phenanthrene was reported to be ~ 5 K.³ Donation of three electrons to an aromatic hydrocarbon molecule was reported to be a key for superconductivity.¹⁻⁶ Very recently, specific heat has also been measured for $Ba_{1.5}$ phenanthrene,^{13,14} which suggests an s-wave, single superconducting gap and an intermediate electron-phonon coupling strength. While the nominal x value (number of metal atoms intercalated) in the superconducting samples of A_x hydrocarbon, AE_x hydrocarbon and Ln_x hydrocarbon (A: alkaline-metal atom, AE: alkaline-earth metal atom, Ln: lanthanide atom) are $x = 3, 1.5$ and 1, respectively, it is imperative to determine the

real x value. Rietveld refinements for X-ray powder diffraction patterns have been extensively used for identifying x in metal-doped C_{60} compounds.¹⁵⁻¹⁷ Since single crystals cannot simply be obtained in the intercalation compounds, the Rietveld refinement is valuable. For the hydrocarbon superconductors, however, the Rietveld refinements have never been achieved because of its low crystal symmetry where the doped metal atoms do not occupy special symmetric sites unlike in the doped C_{60} compounds.

On the other hand, Raman scattering is known to be a powerful tool for determining the x value in A_xC_{60} .¹⁸⁻²⁰ The A_g peak, which is observed at 1469 cm^{-1} for pure C_{60} (with I_h symmetry), shifts to lower frequencies when alkaline metal atoms are doped into C_{60} solids. Actually, the peak shifts by $6 - 7\text{ cm}^{-1}$ for one electron donation to a C_{60} molecule, namely, the A_g peak is observed at 1452 cm^{-1} for K_3C_{60} ,¹⁸ 1448 cm^{-1} for Rb_3C_{60} ¹⁹ and 1447 cm^{-1} for Cs_3C_{60} ,²⁰ providing a good probe for determining the amount of doping. If we now turn to hydrocarbon systems, we previously suggested that some of the peaks shift to lower frequencies with increasing the x value in $K_x\text{picene}$ ² in a similar manner as in A_xC_{60} ,¹⁸⁻²⁰ which indicates that the number of electrons on picene can be determined from the shift of Raman peak from that in pure picene. The number of electrons on phenanthrene molecule in $A_x\text{phenanthrene}$ was successfully determined from the Raman spectrum, which indicates that the superconducting component is $A_3\text{phenanthrene}$. Thus three electron donation seems to be a key for superconductivity,³⁻⁵ but we have definitely to elaborate this. So the first purpose of the present study is to systematically investigate the Raman scattering for $A_x\text{picene}$ (A : K and Rb) to correlate the number of electrons on the hydrocarbon molecules with the Raman frequency. The experimental Raman frequencies have been measured for a wide range of $x = 0 - 5$ in $A_x\text{picene}$, which is compared with theoretical frequencies for the Raman peaks. From this, we have evaluated the number of electrons per picene molecule to clearly determine the x value in the superconducting phases.

Now, in characterizing physical properties of picene superconductors, it is intriguing to compare the picene superconductors with more familiar carbon-based superconductors, *i.e.*, C_{60} and graphite compounds intercalated with alkaline or alkaline earth metal atoms, where the highest T_c to date is 33 K for $RbCs_2C_{60}$ among

C_{60} compounds,²¹ and 11.5 K for CaC_6 among graphite compounds.²² One probe of these materials is the pressure dependence of T_c : indeed, C_{60} and graphite superconductors have opposite tendencies; K_3C_{60} ($T_c = 18$ K) shows a large negative pressure coefficient ($dT_c/dP = -7.8$ K GPa⁻¹),²³ while CaC_6 has a positive one ($dT_c/dP = 0.42 - 0.48$ K GPa⁻¹).²⁴ In the previous paper, we reported briefly the pressure dependence of T_c in 7 K phase of K_3 picene,² but the detailed analysis was not presented. Very recently, positive pressure dependence of T_c in A_x phenanthrene, AE_x phenanthrene and Ln_x phenanthrene was reported,³⁻⁵ which cannot be understood with a simple phonon mechanism of BCS superconductivity. Therefore it is intriguing to examine the pressure dependence of T_c in the $T_c = 7$ and 18 K phases of picene superconductors, which may provide an important key for investigating the mechanism of superconductivity. Thus the second purpose of the present paper is to explore the pressure dependence of 7 K and 18 K phases of K_3 picene, respectively, here reported in a pressure region of 1 bar to 1.2 GPa. We shall show that 18 K phase of K_3 picene has a positive pressure dependence of T_c , while 7 K phase has a negative one. The pressure dependence is discussed from the viewpoints of crystal and electronic structures of picene superconductors.

The third purpose of the present paper is on the fabrication method for K_3 picene samples. A still unclear question is why we have two phases with $T_c = 7$ and 18 K. The usual annealing method (or solid-reaction method) does not allow us to produce selectively 7 or 18 K phases. Even a precise control of nominal composition in K_x picene from $x = 2.6$ to 3.3 produced both 7 K and 18 K superconductors.^{1,2} Here we have prepared K_3 picene superconductor by a solution process with monomethylamine, CH_3NH_2 , as a solvent, in search for a synthetic method for selectively preparing 7 K or 18 K phase. The solution process has previously been used to control polymorphs of Cs_3C_{60} , which is a pressure-induced superconductor ($T_c = 38$ K (A15 phase) and $T_c = 35$ K (face-centered cubic phase) at 15 kbar).^{25,26} Here we shall show that the solution process with CH_3NH_2 for K_3 picene enables us to prepare selectively the K_3 picene sample exhibiting only $T_c = 18$ K.

II. Experimental

Picene (purity: 99.9%) was purchased from NARD Co Ltd., which was used for the experiments without further purification. Alkaline or alkaline earth metal was mixed with picene powder at nominal x value in a pyrex glass tube to fabricate A_x picene. In the annealing method, the pyrex tube was pumped and sealed at 10^{-5} Torr. The tubes were annealed at temperatures as high as ~ 443 K for ~ 10 days. The samples obtained after annealing were black in color. The Raman spectrum and magnetic susceptibility were measured for the samples treated in a glove box without any exposure to air. The Raman scattering was measured at 295 K with Raman spectrometer (JASCO NRS-3100) with an excitation energy having a wavelength $\lambda = 785$ nm, while magnetization, M , was measured with a SQUID magnetometer (Quantum Design MPMS2) in the temperature region > 2 K under ambient and high pressures. A magnetic field, H , of 20 Oe was applied in measuring M/H . For the measurement of pressure dependence of superconductivity, a Cu-Be piston-cylinder type pressure-cell was used. The hydrostatic pressure was mediated by Daphne oil. The applied pressure region was from 1 bar to 1.2 GPa. A small piece of crystalline Sn or Pb was put inside the pressure cell along with the sample to monitor the exact pressure.

In the solution method for preparing A_x picene, on the other hand, CH_3NH_2 was introduced from the CH_3NH_2 gas bottle into the glass vessel containing picene powder and K metal at nominal stoichiometric amounts. The picene and K were completely dissolved in CH_3NH_2 by stirring at 223 K for 3 h. The color of solution was dark-green. After complete dissolution, liquid CH_3NH_2 was removed at 300 K until the base pressure reaches 10^{-4} Torr. The black powder sample obtained after removing CH_3NH_2 was moved into quartz tube in an Ar filled glove box. The tube, dynamically pumped and sealed at 10^{-6} Torr, was annealed at 443 K for 70 h to remove CH_3NH_2 completely. Special care was taken in the annealing procedure because high temperature annealing above 490 K for removal of CH_3NH_2 produces a very toxic material, KCN; actually even below 490 K, KCN may be produced. Powder X-ray diffractions for K_x picene were measured by RIGAKU RINT-TTR III and with synchrotron radiation (KEK-PF, SPring-8 and ESRF). The unit-cell parameters for K_x picene were determined by the LeBail analysis program in GSAS

package.²⁷ Theoretical calculation of Raman frequencies and intensities for A_1 , A_2 , B_1 and B_2 modes for neutral picene and its anions, picene^{y-} ($y = 0 - 5$), with optimized structure (C_{2v} symmetry) was performed with B3LYP program based on hybrid Hartree-Fock (HF) / density functional theory (DFT) with the 6-31G* basis set.²⁸⁻³⁰

III. Results and Discussions

III-1. Characterization of the number of doped metal atoms in K_xpicene and Rb_xpicene

Figures 1(a) and 2(a) show Raman spectra for samples of K_xpicene and Rb_xpicene ($x = 0 - 5$), respectively, at $500 - 1800 \text{ cm}^{-1}$. A pronounced peak at 1378 cm^{-1} marked with an asterisk for pristine picene can be assigned to a superposition of ν_{20} and ν_{21} A_1 vibration modes of picene molecule, where ν_n stands for the n th A_1 vibration mode from the bottom. The ν_{20} and ν_{21} modes in picene^{y-} ($y = 0 - 5$) are schematically depicted in Fig. 3. These vibration modes are suggested to provide strong electron-phonon coupling.⁸ In Figs. 1(b) and 2(b) the theoretical frequencies and intensities of Raman-active A_1 , A_2 , B_1 and B_2 vibration modes are shown along with the experimental Raman spectra, where the experimental peaks are seen to agree well with the theoretical results. Figures 1 and 2 also show that the pronounced peak observed at 1378 cm^{-1} for pristine picene shifts to lower frequencies with an increase in x for both K_xpicene and Rb_xpicene samples.

The average values of ν_{20} and ν_{21} calculated theoretically are plotted for each picene molecule in Figs. 4(a) and (b). The experimental frequencies for the pronounced peak, which are ascribable to superposition of ν_{20} and ν_{21} , are plotted as a function of x for K_xpicene and Rb_xpicene in Figs. 4(a) and (b), respectively. As seen from Fig. 4(a), the experimental frequencies in all the K_xpicene samples basically fall upon three discrete values, 1378 , 1344 and 1313 cm^{-1} , which are consistent with those predicted theoretically for picene, picene^{2-} and picene^{3-} (respective dashed lines). This implies that only two phases, K_2picene and K_3picene , can be produced in

doped K_x picene samples. As for K_1 picene, this separates into two phases, picene and K_2 picene, as seen from Figs. 1(b) and 4(a). The same plots suggest that $K_{1.5}$ picene and K_2 picene samples decompose into three phases, picene, K_2 picene and K_3 picene.

Further, a Raman peak was observed in K_3 picene samples at 1328 cm^{-1} in addition to those for K_2 picene (at 1344 cm^{-1}) and K_3 picene (1313 cm^{-1}), where the value (1328 cm^{-1}) is intermediate between the latter two. Thus the Raman peak at 1328 cm^{-1} may imply the existence of a phase with a fractional x ($K_{2.5}$ picene), although the phase is not a main one. However, two Raman peaks should be observed at 1344 and 1313 cm^{-1} because Raman scattering reflects vibration of molecule even if the $K_{2.5}$ picene phase appears as statistically averaged structure in this sample. Thus the origin of the Raman peak at 1328 cm^{-1} remains to be clarified. If a dynamic conversion of picene²⁻ and picene³⁻ produces the peak at 1328 cm^{-1} , the Raman scattering should be observed at low temperatures with the single peak splitting into peaks at 1344 and 1313 cm^{-1} . When nominal x value was increased above 3, only K_2 picene and K_3 picene were observed, while K_4 picene and K_5 picene phases could not be fabricated, which indicates that the maximum x value is three. From these plots, we conclude that only two phases, K_2 picene and K_3 picene, can be realized by an intercalation of K atoms into picene samples, while K_1 picene is unstable. In Fig. 4(a), the plots for phases with the same x value as the nominal x in the K_x picene sample is indicated in red (e.g., the Raman peak assigned to K_3 picene phase in the K_3 picene sample).

Here, we should stress that the prepared individual K_x picene sample does not always contain all the crystal phases described above, but that some solid samples contain only one or two crystal phases. The number of times the phases appeared is given in parentheses in Fig. 4(a). The numbers then indicate the frequency with which the crystal phases appear. For example, all K_3 picene samples (19 of them) contained the K_3 picene crystal-phase, and 58% in 19 K_3 picene samples showed only a peak ascribable to K_3 picene crystal phase *i.e.*, a single phase of K_3 picene. K_2 picene samples produce a single phase of K_2 picene (20%), picene+ K_2 picene+ K_3 picene phases (20%), a single phase of K_3 picene (20%) and K_2 picene+ K_3 picene (40%). K_1 picene samples resulted in a single phase of K_2 picene (25%) and picene+ K_2 picene phases (75%). $K_{1.5}$ picene samples provided

picene+K₂picene phases (20%), K₂picene+K₃picene (20%) and picene+K₂picene+K₃picene phases (40%) in which each fraction of phase (peak intensity) was almost the same. The K_{1.5}picene samples provided only a single phase of K₂picene (20%). It is suggested from these results that K metal in solid picene may not completely react in most of the samples except for those samples producing a single phase. Judging from the probability, 58%, of realization of the single phase, it is suggested that K₃picene is more stable than K₂picene (25% for a single phase). Therefore, it is of interest to investigate theoretically the energetic stability of K_xpicene phase.

As seen from Figs. 2(b) and 4(b), the ν_{20} , ν_{21} Raman frequencies in Rb_xpicene samples also suggest existence of only three phases (picene, Rb₂picene and Rb₃picene) as in K_xpicene. The observed frequencies, 1378, 1345 and 1313 cm⁻¹, can be assigned to picene, picene²⁻ and picene³⁻, respectively; the values are consistent with those of K_xpicene. It can be concluded from the plots (Fig. 4(b)) that Rb₁picene sample provides only two phases, picene and Rb₂picene, while Rb₂picene and Rb₃picene solid samples provide only three phases (picene, Rb₂picene and Rb₃picene). Thus, increasing nominal x leads to a realization of phases with larger integer x values, in the same manner as in K_xpicene (Fig. 4(a)). Increasing nominal x above 3 produces Rb₃picene and picene as well as a new phase of Rb_{2.5}picene exhibiting a Raman frequency at 1323 cm⁻¹, which was also found in K_xpicene. In the same manner as K_xpicene, the stability of Rb₃picene is confirmed because of high probability, 44%, of formation of a single phase in the Rb₃picene samples.

The magnetic susceptibility has been measured for all the samples of K_xpicene and Rb_xpicene. The $M/H - T$ curves for K_xpicene samples that show the existence of K₃picene phase (with the Raman peak at ~ 1313 cm⁻¹) exhibits a clear drop at 7 or 18 K, indicating superconducting transitions. Conversely, all the samples that have no K₃picene phase exhibit no such behaviors. These results clearly indicate that superconducting phase in K_xpicene relates closely to K₃picene phase. The M/H of Rb_xpicene samples also show the same behavior, *i.e.*, the samples showing the existence of Rb₃picene phase have the superconducting transition, while the Rb₃picene samples that do not exhibit the Raman peak at ~ 1313 cm⁻¹ exhibit no superconducting transitions, indicating that superconducting phase relates to

Rb₃picene. Thus, we have identified that superconducting phases in K_xpicene and Rb_xpicene can be closely associated with K₃picene and Rb₃picene crystal phases, respectively, from the M/H and Raman measurements.

III-2. Pressure dependence of superconducting transition temperature in 7 K and 18 K phases

We now turn to the pressure effect. We first display the $M/H - T$ curves at various pressures for the 7 K phase of K₃picene. Figure 5 shows that the T_c shifts downward with pressure, but only gradually. The midpoint of the superconducting transition, T_c^{mid} , shown in Fig. 5(b), decreases linearly with pressure up to 1 GPa, with $dT_c^{\text{mid}}/dP = -0.3 \text{ K GPa}^{-1}$, which can be determined unambiguously because of the absence of any inhomogeneous broadening of the superconductive transition with increasing pressure. So dT_c/dP of the 7 K phase is negative as in K₃C₆₀, but the coefficient is an order of magnitude smaller. K₃C₆₀ has a three-dimensional (3D) electronic band structure, so that pressure is expected to increase the bandwidth with a decreased density of states at the Fermi energy, $N(\epsilon_F)$,²³ which in turn decreases T_c , regardless of a softening of some C₆₀ vibration modes.³¹ The intercalated graphite, CaC₆, on the other hand, has a positive pressure dependence, where the electronic structure around the Fermi energy is shown to contain a large component of the so-called interlayer states, whose amplitudes reside in between the graphene layers, conferring a 3D character on the electronic structure.^{24,32} In this compound, while the $N(\epsilon_F)$ decreases with pressure, a large softening of an in-plane Ca vibration mode under pressure is shown to cause an increase in the electron-phonon coupling λ , which is considered to overcome the reduction of $N(\epsilon_F)$, leading to an enhanced T_c .

Now we turn to the pressure dependence of T_c in the 18 K phase of K₃picene. Figure 6(a) shows the M/H against T , normalized by the value at 50 K for clarity, for various pressures in the 18 K superconducting phase. We can immediately notice that the T_c^{onset} , shifts *upward*: The T_c^{onset} , shown in Fig. 6(b) against pressure, increases linearly with pressure up to 1.2 GPa, with $dT_c^{\text{onset}}/dP = 12.5 \text{ K GPa}^{-1}$. The large positive pressure dependence found here contrasts sharply with the negative pressure

dependence in the 7 K phase. The positive pressure dependence has also observed in A_3 phenanthrene, $AE_{1.5}$ phenanthrene and Ln_1 phenanthrene.³⁻⁵ However, the size of the coefficient, dT_c^{onset}/dP , is an order of magnitude larger than that, $\sim 1 \text{ K GPa}^{-1}$, of phenanthrene superconductor. Since a reduced volume usually implies a smaller density of states at ϵ_F , this behavior cannot be understood with a simple phonon mechanism of BCS superconductivity.

In K_3 picene, the electronic structure calculation¹⁰ indicates that the interlayer band lies well above the Fermi energy, while the character of the conduction band primarily originates from the LUMO/LUMO+1 orbitals of the picene molecule. More importantly, the wave functions in the conduction band have large amplitudes on the doped K atoms, so that the dopants act not only as a source of charge transfer, but dopant orbits significantly hybridize with the aromatic molecular orbits. Through this mechanism, the coupling between the molecules and dopants should be strong. As reported previously,² when the x value in K_x picene and Rb_x picene is increased, the a -axis is expanded while the b - and c -axes are shrunk, leading to a reduction of unit-cell volume. This implies that the picene molecules become more densely packed when doped with K. This peculiarity comes from a deformation of the in-layer, herringbone arrangement of picene molecules.^{1,2} A theoretical structure optimization¹⁰ indeed indicates that the angle between picene molecules in the herringbone arrangement changes dramatically from 61° to 114° as the metal atoms are doped. These are further indications that the picene molecules and metal atoms form a strongly-knit layer. Thus we expect, first of all, that this will cause the difference in the pressure effect between 7 K and 18 K phases, given the difference in structural phases as described later. The strong coupling between molecules and dopants may also account for the small pressure dependence of T_c in the 7 K phase. Here it should be noticed that T_c ($= 7 \text{ K}$) is invariant in A_3 picene for $A = K$ and Rb ,¹ unlike in fulleride superconductors.³³ The small chemical-pressure effect may also be explained well by the strong coupling described above.

III-3. Selective preparation of 18 K superconducting phase in K_3 picene

Figure 7(a) shows the $MH-T$ curve in zero-field cooling (ZFC) for $K_{3.1}$ picene

sample (nominal $x = 3.1$) that was prepared by the solution process. This data was reported and briefly discussed in Ref. 2. Before annealing the sample or removing CH_3NH_2 from the precursor, the M/H shows a Pauli-like, temperature-independent behavior with a weak increase below 10 K. After the sample is annealed at 443 K for 70 h, the M/H begins to show an abrupt decrease with the $T_c^{\text{onset}} = 18$ K and the $T_c^{\text{mid}} = 17$ K. This superconducting transition coincides with that for the 18 K phase of K_3picene superconductor prepared by solid-reaction method, or annealing method.^{1,2} The maximum shielding fraction is still as low as 0.1%, a value lower by an order of magnitude than that, 1.2 %, for 18 K superconductor prepared by annealing method.¹ However, we notice that the solution-reaction method can produce 18 K superconducting phase more effectively than the solid-state method. In fact all the K_3picene samples prepared by the solution method show a clear decrease in M/H at 18 K. The nominal x value for producing the superconducting phase with the solution process is confined to 2.9 – 3.1, which again suggests that three K atoms per picene molecule is a key doping level.

Figure 7(b) shows Raman scattering spectra for the K_3picene samples prepared by the solution method. One sample (curve A in Fig. 7(b)) was annealed at 443 K for 70 h in vacuum to remove CH_3NH_2 , while the other (curve B) was not annealed. For comparison, the spectra for the K_3picene sample prepared by the solid-reaction method (curve C) as well as for pristine picene (curve D) are also shown. We can see that the Raman spectrum for the $\text{K}_{3.1}\text{picene}$ sample prepared by the solution method (A) coincides with that for the $\text{K}_{3.0}\text{picene}$ prepared by the solid-reaction method (C), where the peak shifts to a lower frequency by 67 cm^{-1} from 1378 cm^{-1} for pristine picene, which suggests that these samples possess the same number of electrons per picene molecule, *i.e.*, these can be represented as K_3picene . This result indicates the effectiveness of annealing at 443 K in vacuum for the removal of CH_3NH_2 , and that CH_3NH_2 molecules are scarcely left in $\text{K}_{3.1}\text{picene}$ sample (A). On the other hand, the peak for the $(\text{CH}_3\text{NH}_2)\text{K}_{3.0}\text{picene}$ sample (B), which was prepared by solution method without annealing, shifts to a lower frequency by 48 cm^{-1} , showing that 2.5 electrons are transferred to picene molecule from K atoms. This implies that the remaining CH_3NH_2 molecule may capture 0.5 electrons from a

picene molecule, *i.e.*, a back-electron transfer from picene molecule.

Figures 8(a) and (b) show X-ray diffraction patterns for the $(\text{CH}_3\text{NH}_2)_2\text{K}_3\text{picene}$ and K_3picene samples, respectively. The former was prepared by the solution method without annealing, while the latter was prepared by the solution method with annealing at 443 K for 70 h. The lattice parameters for the two samples obtained from the LeBail fit to X-ray diffraction patterns (Fig. 8) are listed in table 1; the space group was assumed to be $P2_1$ in these samples, in the same manner as picene and K_3picene prepared by solid reaction method.^{1,2} We can see from this table that the lattice parameters, a and c , for the K_3picene sample prepared by the solution method without annealing increase from those in pristine picene. Specifically, the c axis expands markedly, suggesting that CH_3NH_2 molecules are mainly intercalated into the space between the herringbone (ab -plane) layers of picene molecules.

The values of a and c in the K_3picene sample, prepared by the solution method with annealing, are smaller than those in the sample without annealing, which indicates that CH_3NH_2 was basically removed in the sample annealed at 443 K in vacuum, as consistent with the results obtained from the Raman scattering. The K_3picene sample prepared by the solid reaction (C in Fig. 7(b)) showed T_c of 7 K, while the K_3picene sample (A in Fig. 7(b)) prepared by the solution method with annealing showed T_c of 18 K. All the lattice parameters in the K_3picene sample prepared by the solution method with annealing are larger than those in pure picene, especially the c expands, suggesting that the crystal structure of K_3picene phase prepared by solution method is different from that (7 K phase) prepared by the solid reaction, *i.e.*, the K atoms in K_3picene prepared by the solution method may be intercalated into the space between ab -layers.

In fact, the theoretical calculation^{10,34,35} (as summarized in table 2 for the structure parameters) shows an existence of two kinds of doping structures: (i) the one (denoted as K_3picene) with the dopants inserted within the herringbone-arranged picene layer (ab -layer), and (ii) another with some dopants intercalated in the interlayer regions as well, where the latter is meta-stable but does exhibit a local energy minimum. The structure is denoted as $\text{K}_2\text{K}_1\text{picene}$ where two K atoms are inserted into the ab -layer while one K atom is intercalated into the space between ab -layers.^{2,10} The lattice constants determined by X-ray diffraction indicate the

expansion of a -axis and shrinkage of c -axis in the 7 K phase prepared by solid reaction, suggesting the intercalation of K atoms into the picene layer (ab -layer), which is consistent with the location of K atoms with intralayer insertion obtained theoretically.¹⁰ On the other hand, some of the K atoms in K_3 picene prepared by solution method may be intercalated into the space between ab -layers, which is consistent with the theoretical prediction that the structure with both intralayer and interlayer dopants is a meta-stable structure.^{10,34,35} Thus the theoretical structure (K_2K_1 picene with two intra-layer and one inter-layer picene molecules) may possibly be related to the 18 K phase prepared by solution method, but this definitely requires further confirmation.

Superconducting mechanism and the symmetry of the gap function have yet to be known. The previous theoretical calculation suggests that the electron-phonon coupling is sufficiently strong to roughly account the size of T_c in doped picene.^{8,9,36} At the same time, however, a possible relevance of the strong electron-electron correlation is pointed out in other theoretical works.³⁷⁻³⁹ The multiple structures, found here to be dependent on the sample fabrication method, is consistent with the previous theoretical suggestion that there are multiple meta-stable structures in the doped picene.^{10,34,35} More importantly, if the identification of the 18 K phase of the superconductivity to be the structure with the intralayer plus interlayer insertion of dopants is correct, this implies the superconductivity is dominated by details in the doping structure, and this may give a crucial clue in exploring the superconductivity mechanism, including some unconventional ones. Indeed, here we find that the 7 K and 18 K phases react in opposite manners against the applied pressure, which may provide an important test in sorting the mechanism. The first thing we should check theoretically is how the density of states (DOS) changes against pressure. As shown theoretically^{10,34,35}, the conduction band comprises multiple orbitals, so that the DOS may show a nontrivial dependence on the pressure. The next interest is how the shape of the Fermi surface, which can be crucial in unconventional superconductivity, changes against pressure. This is interesting, since even at ambient pressure the Fermi surface is shown to be a composite of pieces with different dimensionalities^{10,34,35}. Such a study is under way, and will be reported elsewhere.

IV. Summary and discussion

The conclusion of the present paper is three-fold: (i) We have performed a characterization of the number of electrons on picene molecule by use of Raman scattering, and two different phases of A_2 picene and A_3 picene were found in the A_x picene samples, indicating the absence of A_1 picene phase. From the Raman scattering of superconducting A_x picene samples, it has been found that the A_3 picene phase relates closely to superconducting phase. (ii) The pressure study revealed that the 18 K phase has a positive dT_c^{mid}/dP as in superconducting phenanthrene³⁻⁵, while the 7 K phase has a negative coefficient. The latter is understandable from the BCS picture, while the former does not fit with a simple phonon-mechanism BCS superconductivity. (iii) The preparation of K_3 picene by a solution method led selectively to 18 K superconducting phase, which is different from the preparation by annealing method which produces 7 or 18 K phase. The K_3 picene sample prepared by the solution method showed longer c axis than in K_3 picene with the annealing method, indicating that the K atoms may be intercalated into the space between the herringbone (ab) layers.

As for the metallicity of the system, Refs. 40,41 report photoemission results for a vanishing density of states at the Fermi energy, suggestive of an insulating state of the doped picene. However, it has also been found that the photoemission spectrum for pristine picene films significantly varies according to the substrate used,⁴⁰ which suggests that the growth orientation of molecules and/or the crystal structure may depend on the substrate, and this may account for the difference in the electronic states (metallic or insulating) in doped picene. Theoretically, Ref. 41 suggests that K-doped picene systems are insulating for all the stoichiometric filling n on the basis of DFT + DMFT calculation. One possible explanation for this discrepancy, apart from the possible difference in the film structure mentioned above, is that the Hubbard $U = 1.6$ eV⁴¹, extracted from a molecular based calculation³⁷, is considerably larger than $U \sim 0.8$ eV estimated with the constrained random phase approximation³⁹. The precise value of U may be important, since, according to Ref. 41 the metal-insulator transition takes place around $U = 0.6-0.8$ for K_3 picene. If the actual U value is on the Mott insulating side, the observed metallicity may come

from a small deviation of the filling n from an integer value.

Thus, with the present study opening up a new synthesis route for producing the crystal phase (K_3 picene) exhibiting the 18 K superconducting transition, the correlation of the electronic structure with the arrangement of molecules and doping level should be an interesting future problem.

Acknowledgment. The authors appreciate to Takayoshi Yokoya and Hiroyuki Okazaki for valuable discussions on the photoemission study, Masaki Mifune of Department of Pharmaceutical Science, Okayama University, for his valuable assistance in the Raman measurement. HA is benefitted from discussions with Taichi Kosugi of AIST. This study is partly supported by Grant-in-aid (23340104, 23684028, 22244045, 24654105) of MEXT, by the LEMSUPER project (JST-EU Superconductor Project) in Japan Science and Technology Agency (JST), and by Special Project of Okayama University / MEXT. The X-ray diffractions with synchrotron radiation were done under the proposals of KEK-PF (2011G109), SPring-8 (2011A1938) and ESRF (HS-4556).

References

1. R. Mitsuhashi, Y. Suzuki, Y. Yamanari, H. Mitamura, T. Kambe, N. Ikeda, H. Okamoto, A. Fujiwara, M. Yamaji, N. Kawasaki, Y. Maniwa, Y. Kubozono, *Nature* 464, 76 (2010).
2. Y. Kubozono, H. Mitamura, X. Lee, X. He, Y. Yamanari, Y. takahashi, Y. Suzuki, Y. Kaji, R. Eguchi, K. Akaike, T. Kambe, H. Okamoto, A. Fujiwara, T. kato, T. Kosugi, H. Aoki, *Phys. Chem. Chem. Phys.* 13, 16476 (2011).
3. X. F. Wang, R. H. Liu, Z. Gui, Y. L. Xie, Y. J. Yan, J. J. Ying, X. G. Luo, X. H. Chen, *Nature Commun.* 2, 507 (2011).
4. X. F. Wang, Y. J. Yan, Z. Gui, R. H. Liu, J. J. Ying, X. G. Luo, X. H. Chen. *Phys. Rev. B.* 84, 214523 (2011).
5. X. F. Wang, X. G. Luo, J. J. Ying, Z. J. Xiang, S. L. Zhang, R. R. Zhang, Y. H. Zhang, Y. J. Yan, A. F. Wang, P. Cheng, G. J. Ye, X. H. Chen, *J.Phys.:Condens. Matter*, 24, 345701(2012).
6. M. Xue, T. Cao, D. Wang, Y. Wu, H. Yang, X. Dong, J. He, F. Li, G. F. Chen, *Scientific Reports*, 2, 389; DOI: 10.1038/srep00389 (2012).
7. J. E. Schirber, D. L. Overmyer, K. D. Carlson, J. M. Williams, A. M. Kini, H. Hau Wang, H. A. Charlier, B. J. Love, D. M. Watkins, G. A. Yaconi, *Phys. Rev. B* 44, 4666 (1991).
8. T. Kato, T. Kambe, Y. Kubozono, *Phys. Rev. Lett.*, 107, 077001 (2011).
9. M. Casula, M. Calandra, G. Profeta, F. Mauri, *Phys. Rev. Lett.* 107, 137006 (2011).
10. T. Kosugi, T. Miyake, S. Ishibashi, R. Arita, H. Aoki, *J. Phys. Soc. Jpn.* 78, 113704 (2009).
11. H. Okazaki, T. Wakita, T. Muro, Y. Kaji, X. Lee, H. Mitamura, N. Kawasaki, Y. Kubozono, Y. Yamanari, T. Kambe, T. Kato, M. Hirai, Y. Muraoka, T. Yokoya, *Phys. Rev. B*, 82,195114 (2010).
12. K. Teranishi, X. He, Y. Sakai, M. Izumi, H. Goto, R. Eguchi, Y. Takabayashi, T. Kambe, Y. Kubozono, unpublished.
13. J. Ying, X. Wang, Y. Yang, Z. Xiang, X. Luo, Z. Sun, X. Chen, *Phys. Rev. B* 85, 180511(R) (2012).
14. Y. Kasahara, Y. Takeuchi, Y. Iwasa, *Phys. Rev. B* 85, 214520 (2012).

15. P. W. Stephens, L. Mihaly, P. L. Lee, R. L. Whetten, S.-M. Huang, R. Kaner, F. Diederich, K. Holczer, *Nature*, 351, 632 (1991).
16. O. Zhou, D. E. Cox, *J. Phys. Chem. Solids* 53, 1373 (1992).
17. C. A. Kuntscher, G. M. Bendele, P. W. Stephens, *Phys. Rev. B* 55, R3366 (1997).
18. T. Pichler, M. Matus, J. K rti, H. Kuzmany, *Phys. Rev. B* 45, R13841 (1992).
19. M. S. Dresselhaus, G. Dresselhaus, P. C. Eklund, *J. Raman Spectros.* 27, 351 (1996), and references therein.
20. S. Fujiki, Y. Kubozono, S. Emura, Y. Takabayashi, S. Kashino, A. Fujiwara, K. Ishii, H. Suematsu, Y. Murakami, Y. Iwasa, T. Mitani, H. Ogata, *Phys. Rev. B* 62, 5366 (2000).
21. K. Tanigaki, T. W. Ebbesen, S. Saito, J. Mizuki, J. S. Tsai, Y. Kubo, S. Kuroshima, *Nature*, 352, 222 (1991).
22. N. Emery, C. H rold, M. d'Astuto, V. Garcia, Ch. Bellin, J. F. Mar che, P. Lagrange, G. Loupiau, *Phys. Rev. Lett.*, 95, 087003 (2005).
23. G. Sparrn, J. D. Thompson, S.-M. Huang, R. B. Kaner, F. Diederich, R. L. Whetten, G. Gr uner, K. Holczer, *Science*, 252, 1829 (1991).
24. J. S. Kim, L. Boeri, R. K. Kremer, F. S. Razavi, *Phys. Rev. B* 74, 214513 (2006).
25. A. Y. Ganin, Y. Takabayashi, Y. Z. Khimyak, S. Margadonna, A. Tamai, M. J. Rosseinsky, K. Prassides, *Nature Mater.* 7, 367 (2008).
26. Y. Takabayashi, A. Y. Ganin, P. Jegli , D. Ar on, T. Takano, Y. Iwasa, Y. Ohishi, M. Takata, N. Takeshita, K. Prassides, M. J. Rosseinsky, *Science*, 323, 1585 (2009).
27. A.C. Larson and R.B. Von Dreele, "General Structure Analysis System (GSAS)", Los Alamos National Laboratory Report LAUR 86-748 (2004).
28. A. D. Becke, *Phys. Rev. A* 38, 3098 (1988).
29. C. Lee, W. Yang, R. G. Parr, *Phys. Rev. B* 37, 785 (1988).
30. R. Ditchfield, W. J. Hehre, J. A. Pople, *J. Chem. Phys.* 54, 724 (1971).
31. D. W. Snoke, Y. S. Raptis, K. Syassen, *Phys. Rev. B* 45, 14419(1992).
32. G. Cs nyi, P. B. Littlewood, A. H. Nevidomskyy, C. J. Pickard, B. D. Simons, *Nature Phys.* 1, 42 (2005).
33. R. M. Fleming, A. P. Ramirez, M. J. Rosseinsky, D. W. Murphy, R. C. Haddon, S. M. Zahurak, A. V. Makhija, *Nature* 352, 787 (1991).
34. T. Kosugi, T. Miyake, S. Ishibashi, R. Arita, H. Aoki, *Phys. Rev. B* 84, 214506

(2011).

35. T. Kosugi, T. Miyake, S. Ishibashi, R. Arita, H. Aoki, Phys. Rev. B 84, 020507(R) (2011).

36. A. Subedi and L. Boeri, Phys. Rev. B 84, 020508(R) (2011).

37. G. Giovannetti and M. Capone, Phys. Rev. B 83, 134508 (2011).

38. M. Kim, B. I. Min, G. Lee, H. J. Kwon, Y. M. Rhee, J. H. Shim, Phys. Rev. B 83, 214510 (2011).

39. Y. Nomura, K. Nakamura, R. Arita, Phys. Rev. B 85, 155452 (2012).

40. B. Mahns, F. Roth, M. Knupfer, J. Chem. Phys., 136, 134503 (2012).

41. A. Ruff, M. Sing, R. Claessen, H. Lee, M. Tomić, H. O. Jeschke, R. Valentí, arXiv:1210.4065.

Table 1. Experimentally obtained lattice parameters for picene and K-doped picene.

	a (Å)	b (Å)	c (Å)	β (°)	$V(\text{Å}^3)$
Pristine picene ^{a)}	8.472(2)	6.170(2)	13.538(7)	90.81(4)	708
K ₃ picene ^{b)}	8.707(7)	5.912(4)	12.97(1)	92.77(5)	667
(CH ₃ NH ₂) ₂ K ₃ picene ^{c)}	8.927(5)	6.151(1)	14.476(4)	94.16(3)	793
K ₃ picene ^{d)}	8.571(5)	6.270(2)	14.001(3)	91.68(3)	752

a) Taken from ref. 1.

b) Taken from ref. 1, where the sample was prepared by solid reaction method.

c) Sample prepared by solution method without annealing.

d) Sample prepared by solution method with annealing.

Table 2. Theoretically obtained lattice parameters for K-doped picene.³⁴ K₃picene stands for a structure where all the three K atoms are inserted within the picene layer (with two possible structures A and B), while K₂K₁picene a structure with two intralayer atoms and one interlayer one.

	a (Å)	b (Å)	c (Å)	β (°)	$V(\text{Å}^3)$
K ₂ K ₁ picene	8.776	6.394	13.346	94.03	747.069
K ₃ picene (A)	7.421	7.213	14.028	104.53	726.848
K ₃ picene (B)	7.408	7.223	14.116	105.93	726.328

Figure captions

Fig. 1. Raman scattering spectra in K_x picene ($x = 0 - 5$) at (a) $500 - 1800 \text{ cm}^{-1}$ and (b) $1250 - 1400 \text{ cm}^{-1}$. Raman peaks calculated theoretically are indicated with bars in (b) with A_1 (B_2) mode in red (blue). The height of the red bars represents the relative intensities of the Raman peak. All the theoretical results are shifted downward by 27 cm^{-1} so that the theoretical average value of ν_{20} and ν_{21} A_1 modes in neutral picene fits to its experimental average value, 1378 cm^{-1} . The arrows indicate averaged values of theoretical ν_{20} and ν_{21} A_1 modes. The explanation of notation, ν_n , is described in text.

Fig. 2. A similar plot as in Fig.1 for Rb_x picene ($x = 0 - 5$).

Fig. 3. ν_{20} and ν_{21} A_1 modes schematically shown for picene^y ($y = 0 - 5$).

Fig.4. Plots of frequency of experimental and theoretical Raman peaks against the nominal value, x , in (a) K_x picene and (b) Rb_x picene ($x = 0 - 5$). Frequency of the theoretical Raman peak corresponds to the average value of frequencies for ν_{20} and ν_{21} A_1 modes. The theoretical plots are shifted by 27 cm^{-1} so that the theoretical average value of ν_{20} and ν_{21} A_1 modes in neutral picene fits to its experimental average value, 1378 cm^{-1} . The experimental plots in red refer to the K_x picene (Rb_x picene) phase produced in the K_x picene (Rb_x picene) sample (see text). The numerical value in parenthesis stands for the number of times the phase appeared in each sample.

Fig. 5. (a) $M/H - T$ curves for various pressures, and (b) pressure dependence of T_c^{mid} in the 7 K superconducting phase of $K_{3.3}$ picene. dT_c^{mid}/dP is determined by a linear fitting in $T_c^{\text{mid}} - P$ plot.

Fig. 6. Similar plot as in Fig.5 for the 18 K superconducting phase of $K_{3.3}$ picene.

Fig. 7 (a) $M/H - T$ curve in zero-field cooling (ZFC) for $(\text{CH}_3\text{NH}_2)\text{K}_3$ picene and $\text{K}_{3.1}$ picene samples, which were prepared by the solution process (see text). This data was reported and briefly discussed in ref. 2. (b) Raman scattering spectra for the

K₃picene samples which were prepared by the solution method (curve A), (CH₃NH₂)K₃picene (curve B), K₃picene sample prepared by the solid-reaction method (curve C), and pristine picene (curve D).

Fig. 8. X-ray diffraction patterns for (a) (CH₃NH₂)K₃picene and (b) K₃picene samples. Red circles (blue lines) represent the observed (calculated) diffraction patterns. The green line shows the difference between the observed and calculated patterns. Black vertical bars correspond to the predicted peak positions. The lattice parameters for two samples, (CH₃NH₂)K₃picene and K₃picene, obtained from the LeBail fit to X-ray diffraction patterns are listed in Table 1.

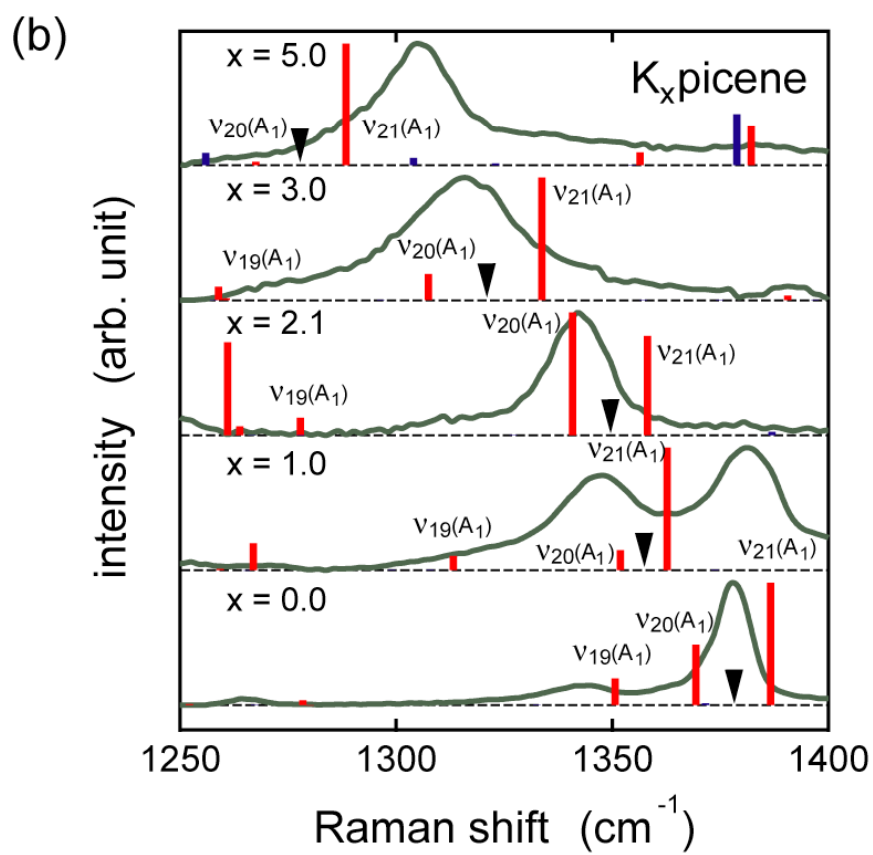
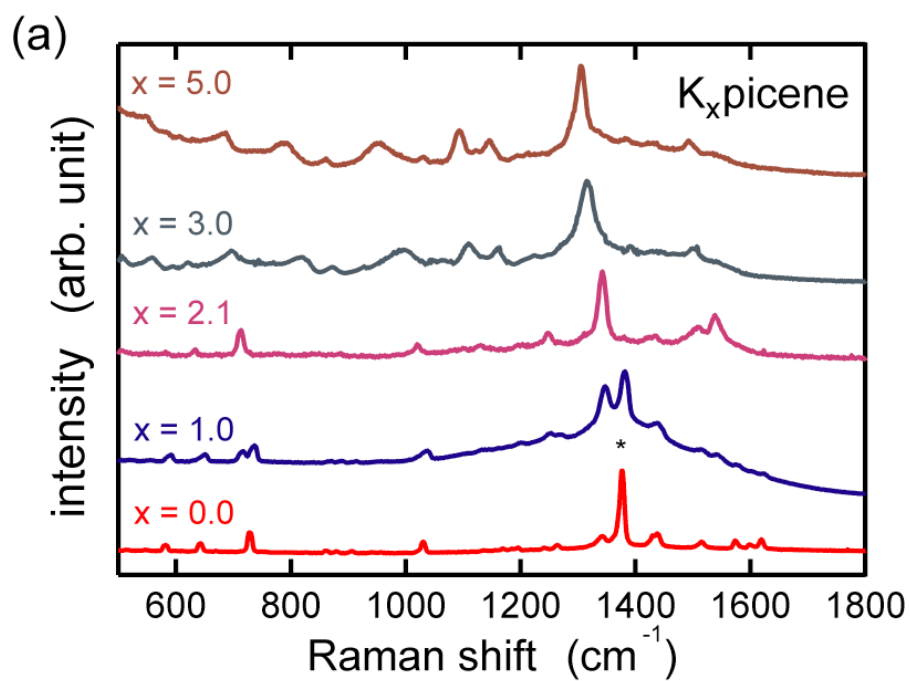


Figure 1. T. Kambe et al.,

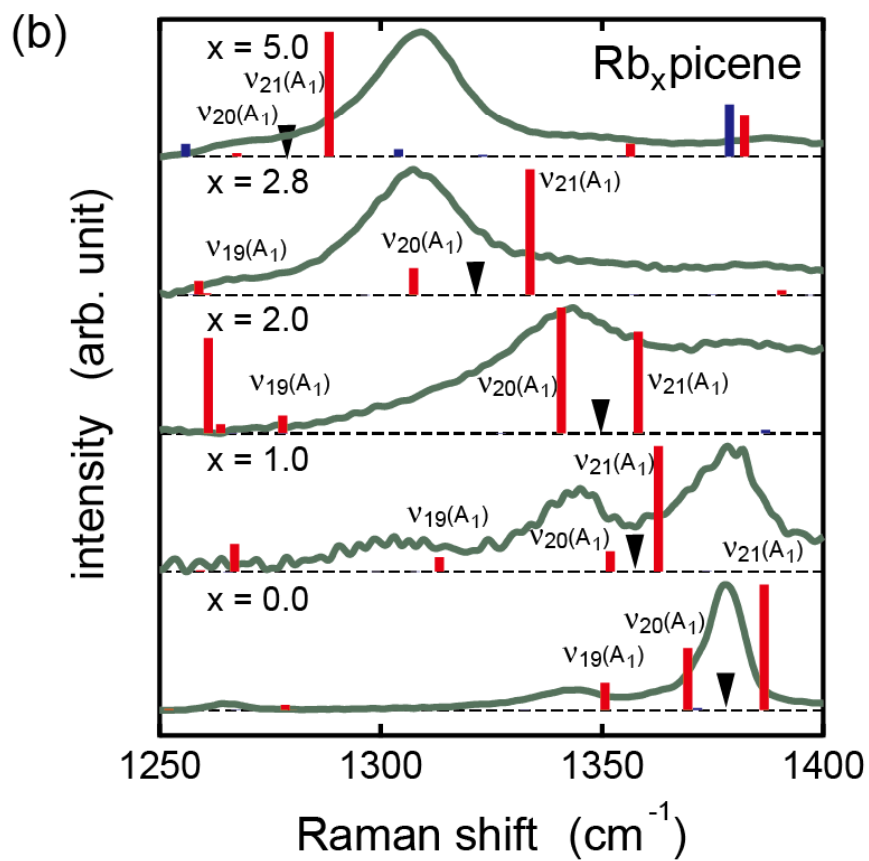
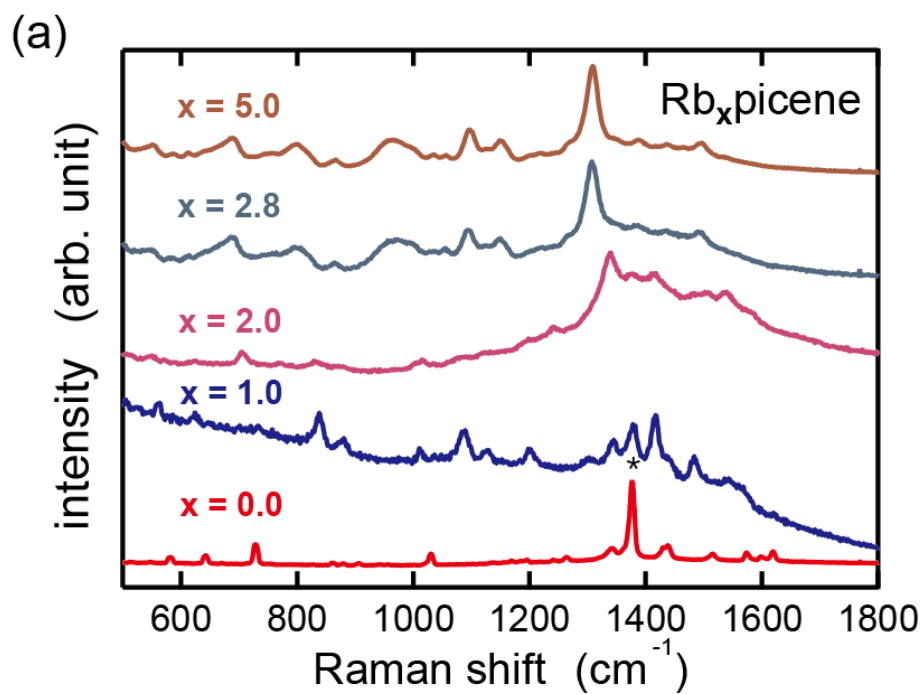


Figure 2. T. Kambe et al.,

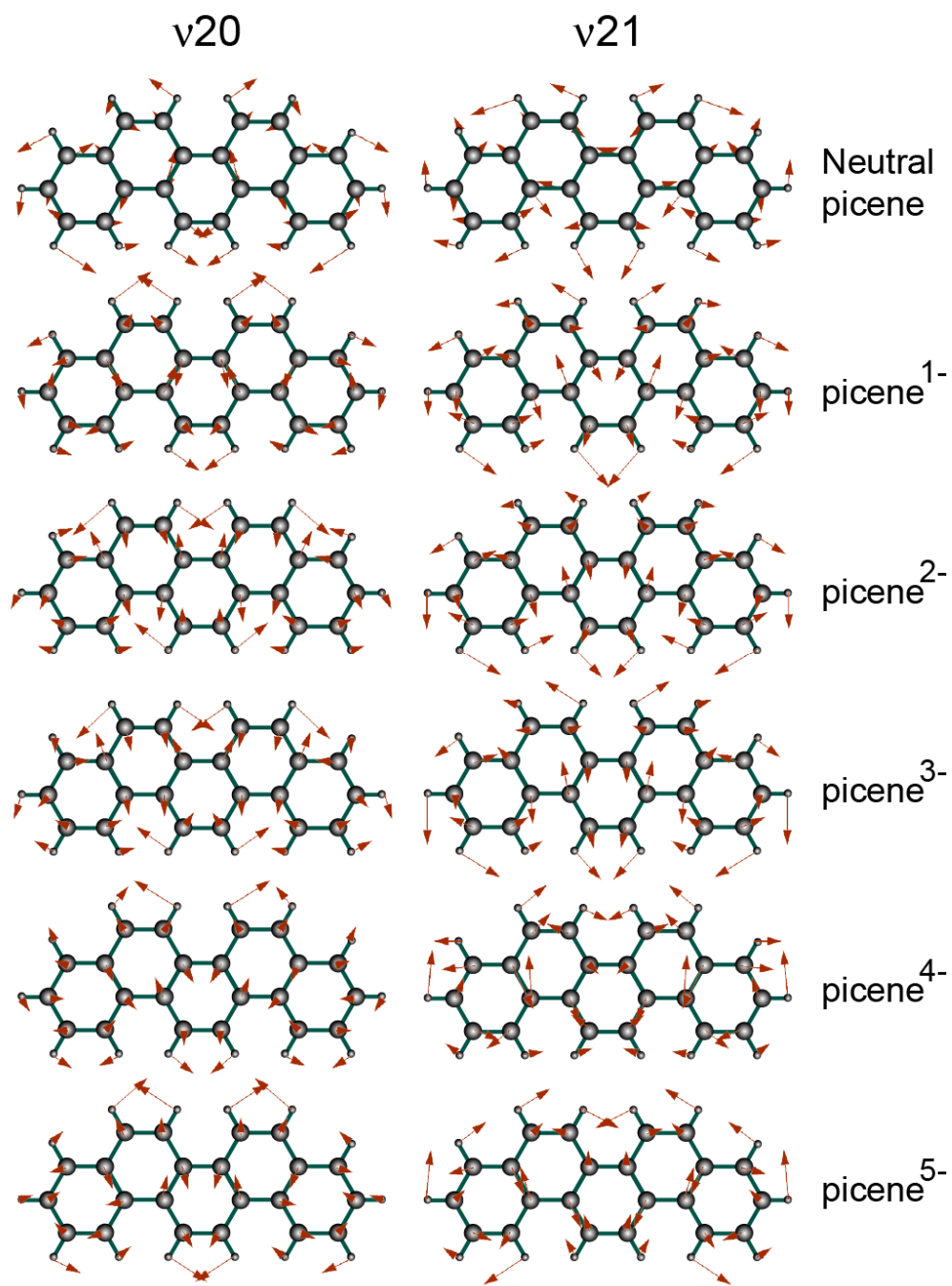


Figure 3. T. Kambe et al.,

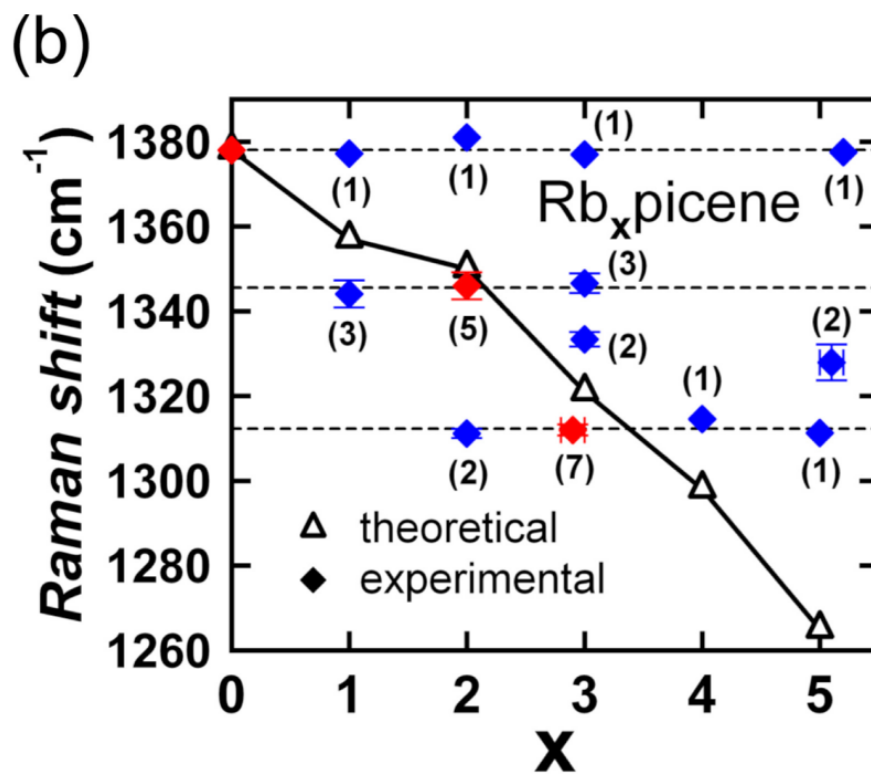
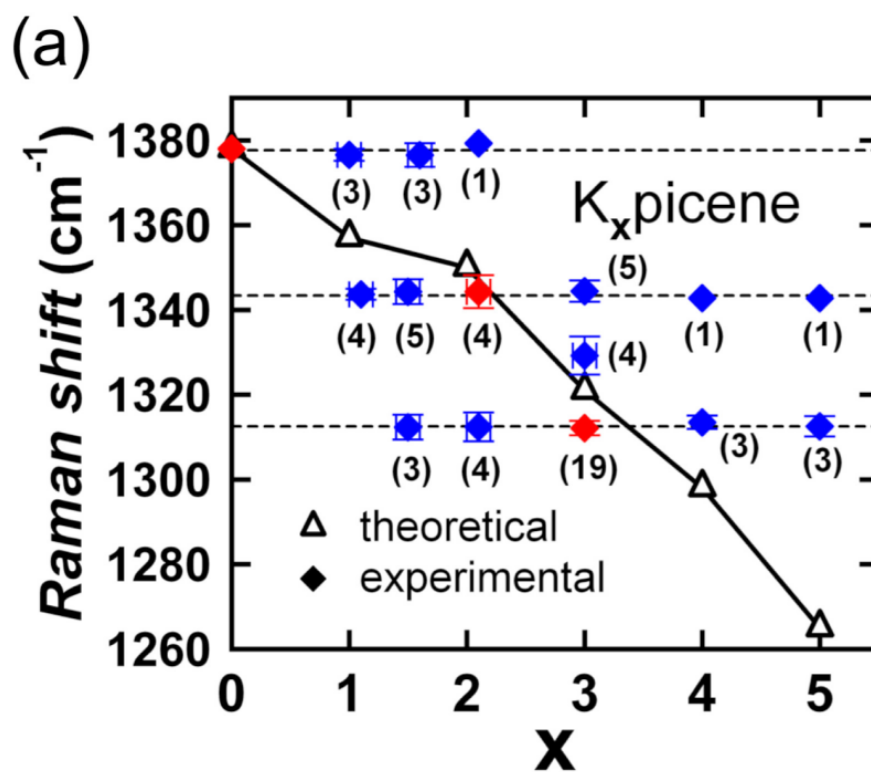


Figure 4. T. Kambe et al.,

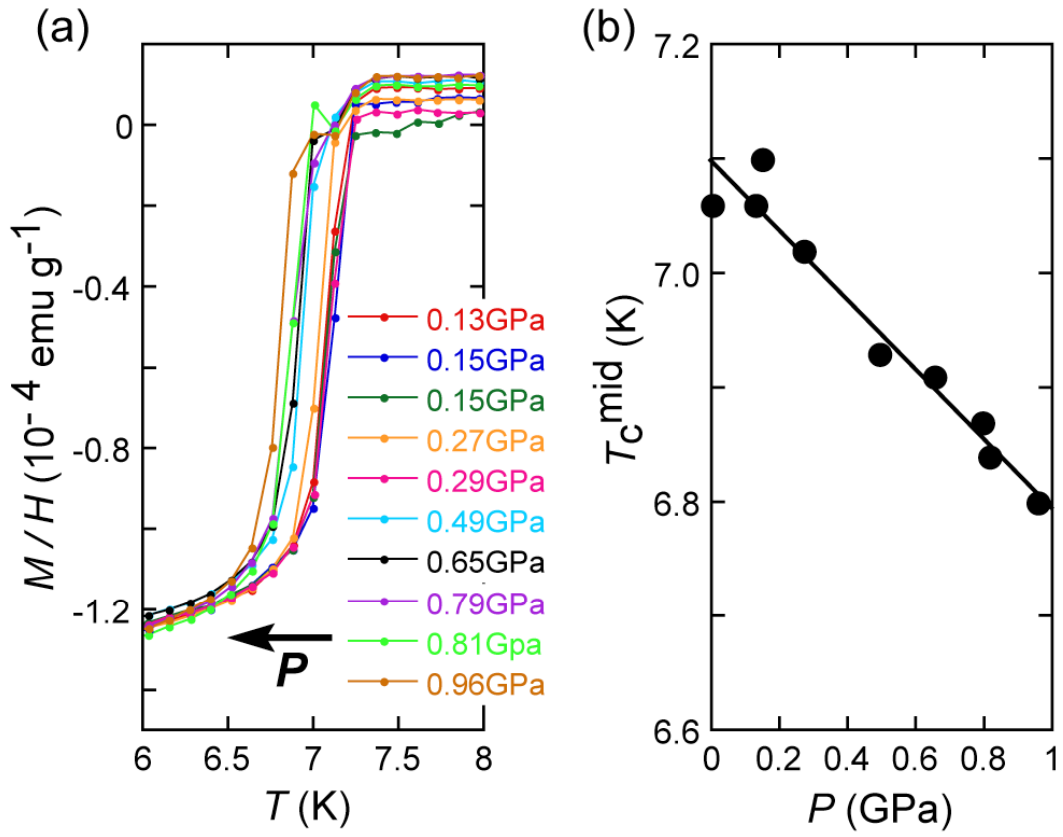


Figure 5. T. Kambe et al.,

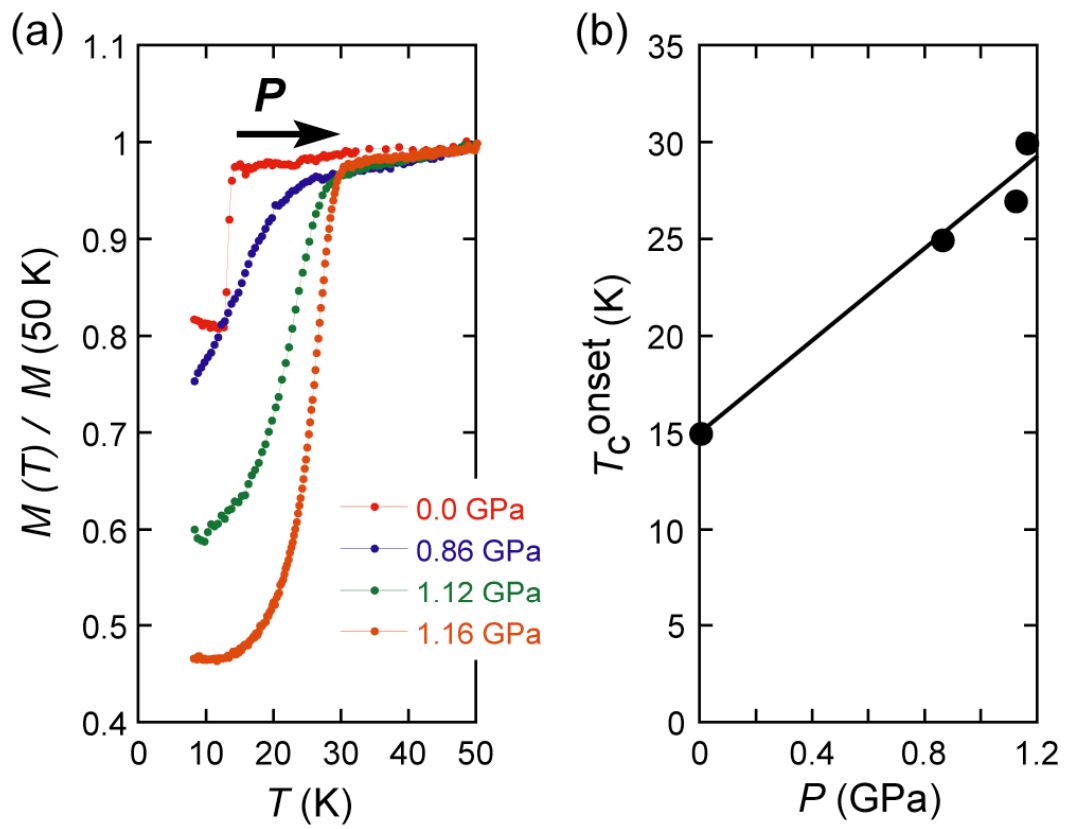


Figure 6. T. Kambe et al.,

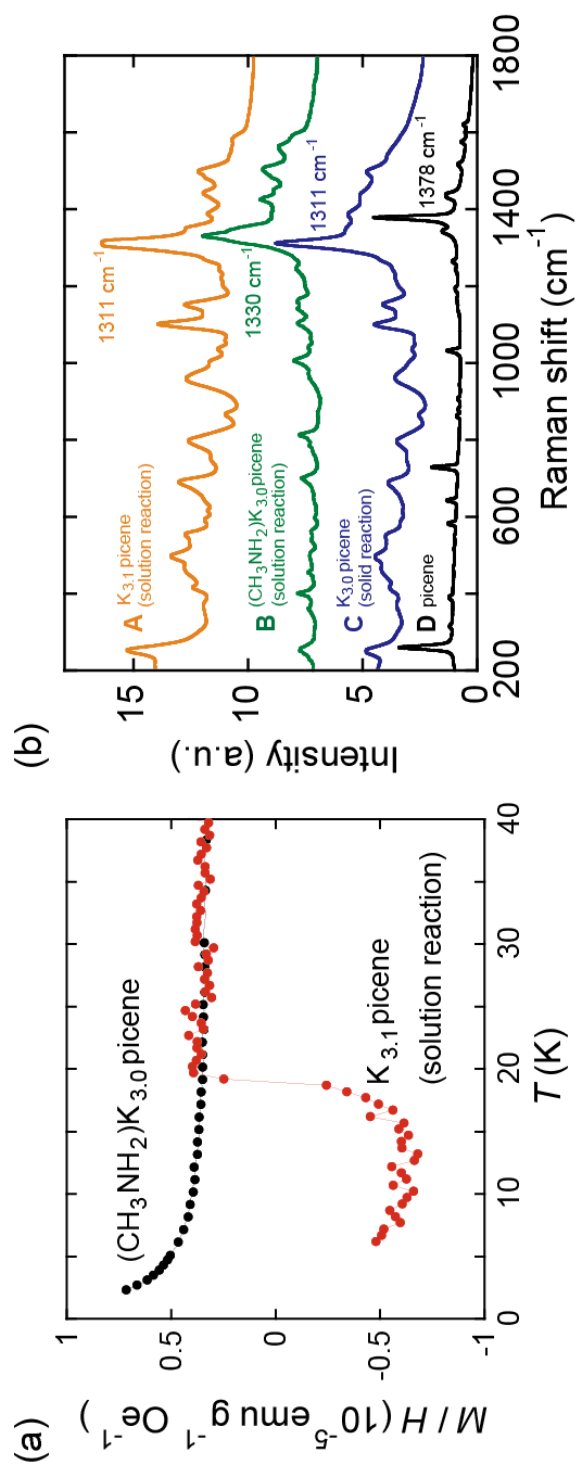


Figure 7. T. Kambe et al.,

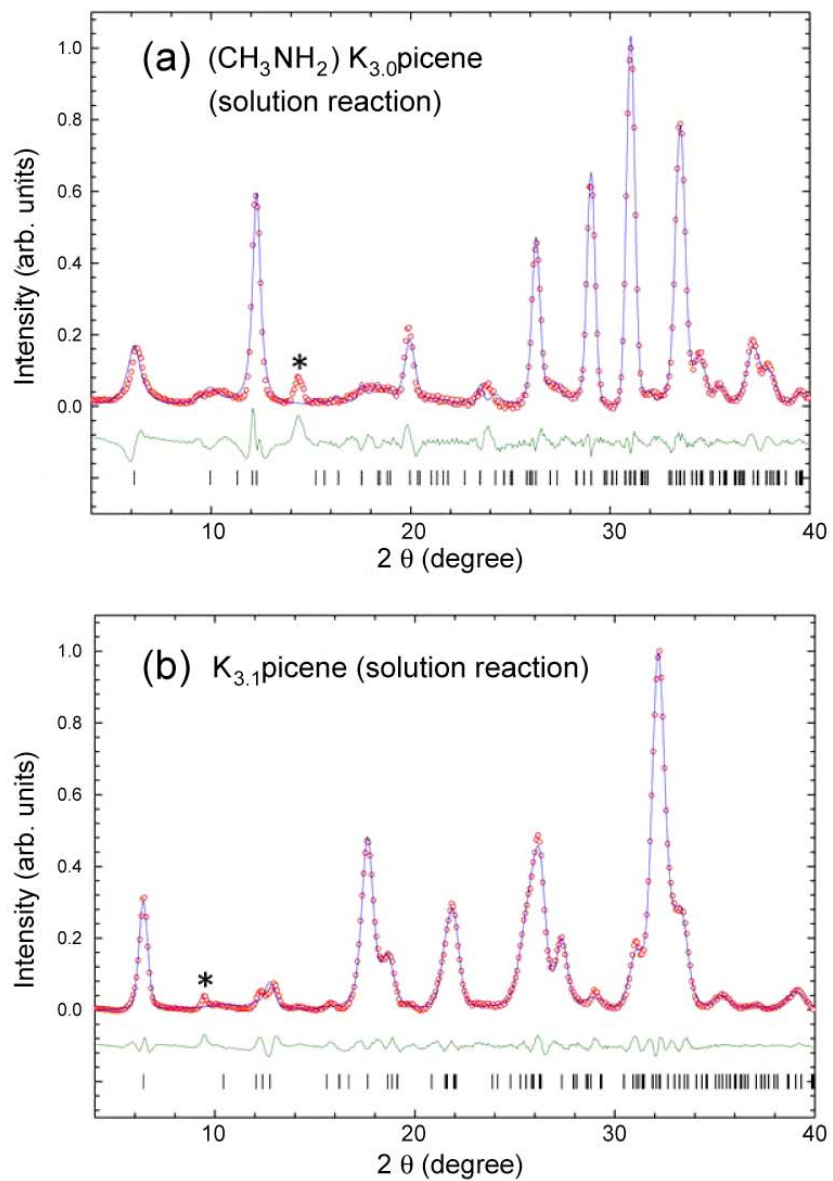


Figure 8. T. Kambe et al.,